IN-SITU ATMOSPHERIC PROFILES FROM MARS ENTRY CAPSULE HEAT SHIELD PRESSURE INSTRUMENTATION

B. Van Hove, *Royal Observatory of Belgium, Ukkel, Belgium (bartvh@observatory.be)*, **Ö. Karatekin**, (*o.karatekin@observatory.be).*

Introduction:

Atmospheric entry, descent, and landing (EDL) is an opportunity to make scientific observations of the in-situ atmospheric conditions on Mars. Density, pressure, and temperature can be derived from engineering data recorded during flight, along the EDL trajectory. Benefits of these atmospheric profiles are their large vertical range and high spatial resolution, able to capture local atmospheric fluctuations that are difficult to observe remotely.

Conventionally, atmospheric reconstruction with flight data is based on measurements of the vehicle angular rate and aerodynamic acceleration, recorded by an inertial measurement unit (IMU). The main drawback of this approach is that density is derived from acceleration data by assuming an aerodynamic drag coefficient [1–2]. This propagates uncertainty on aerodynamics modeling straight to the atmospheric reconstruction, in which pressure and temperature are also based on this potentially biased density. According to [3], uncertainty on aerodynamics models can be as high as 14% (3-σ).

This issue can be overcome by recording the pressure on the vehicle heat shield, in addition to IMU data. Heat shield surface pressures are correlated with atmospheric density, and can be interpreted without aerodynamics models. Only a few Mars entry vehicles have been equipped with heat shield pressure instrumentation so far, of which the 2012 Mars Science Laboratory (MSL) returned the most complete and accurate pressure flight data.

At this workshop we will present an atmospheric reconstruction along the MSL entry trajectory, based strongly on heat shield pressure data. Studies of MSL pressure data in literature [4–6] have reconstructed atmospheric conditions, wind-relative attitude, and aerodynamic performance using pressure data from seven locations on the heat shield, see Fig. 1, and pressure models of corresponding complexity. We will consider pressure measurements from a single pressure sensor to obtain atmospheric conditions directly. This reduces demands on the pressure model used to convert pressures to atmospheric density, where we employed a 1-D equilibrium flow model. Because the model is 1-D and does not consider non-equilibrium chemistry, it is valid for any blunted heat shield geometry, and a large range of Mars trajectory conditions. We demonstrate this by comparison with atmospheric conditions obtained in the multiple sensor reconstruction in [4], and show that the present method is accurate and could be applied to a wide range of Mars EDL trajectory conditions. We also compare the present atmospheric reconstruction to predictions from a global circulation model for Mars, from the Mars Climate Database (MCD).

Background:

Initial attempts to measure heat shield pressures during Mars entry with the Viking landers in 1967, were only partly successful [7–8]. Pressure data from Viking 1 were used for atmospheric reconstruction [9–10], but not sufficiently accurate to separate aerodynamic and atmospheric uncertainties [11–12]. Subsequent pressure data were obtained only much later by the MSL entry vehicle, which successfully landed the Curiosity rover in August 2012 [5]. The Schiaparelli lander of the 2016 ExoMars mission also recorded heat shield pressure data, but at the time of writing these measurements are still pending validation. Based on MSL post-flight analysis and hardware calibrations [13], the MSL pressure data will likely remain the most accurate such measurements for Mars so far. MSL pressure data were converted to engineering units and tabulated in [14].

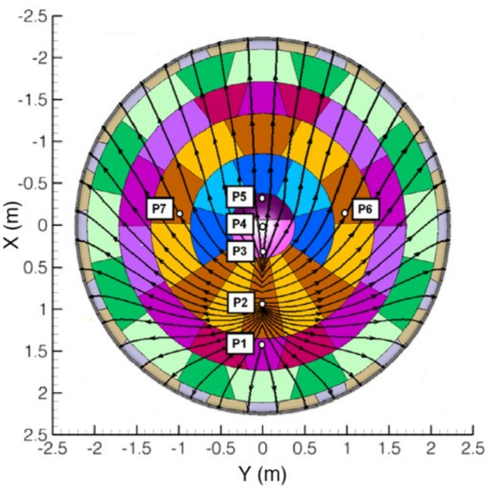

Fig. 1 MSL pressure sensors looking at the heat shield, streamlines show an example flowfield predicted by CFD, extracted from [13].

The pressure distribution on a blunt entry vehicle reaches a local maximum, referred to as *stagnation pressure*. Fig. 1 shows an example pressure distribution on the MSL heat shield. Seven MSL pressure sensors are shown, and sensor P2 is closest to the stagnation point where several streamlines converge. Remaining pressure sensors farther away from the stagnation point are more sensitive to vehicle attitude, and intended to observe aerodynamic performance. This requires models of the entire pressure distribution, obtained by wind tunnel testing or 3-D Navier-Stokes computational fluid dynamics (CFD). For MSL, CFD modeling included complex physics such as non-equilibrium gas chemistry, convective and radiative heat transfer, viscosity, boundary layer behavior… which are specific to MSL geometry and trajectory conditions.

While the entire and detailed heat shield pressure distribution depends on many parameters (attitude, geometry…) the stagnation pressure is expected to be much less sensitive to these factors [15]. In the present work, we demonstrate a method that employs a 1-D flow model with equilibrium gas chemistry, based on classical normal shock wave relations but considering high-temperature effects. The model is used to convert MSL pressure data from near the stagnation point to atmospheric density, from which pressure and temperature are derived in an iterative process. Results will be evaluated by comparison with the 'MEADS reconstruction' from [4], where data from all seven sensors was fitted to 3-D flowfield solutions from CFD, described above. Atmospheric reconstruction results will be analyzed further by comparison with the MCD atmospheric model.

Method:

The normalized stagnation pressure coefficient is defined as

$$C_{pt2} = \frac{p_{t2} - p_\infty}{\frac{1}{2}\rho_\infty V_\infty^2} \tag{1}$$

with stagnation pressure p_{t2}, atmospheric pressure p_∞, density ρ_∞,, and atmosphere relative velocity V_∞. The magnitude of C_{pt2} is required to use Eq. (1) for density reconstruction from p_{t2} flight data. Dynamic pressure in the denominator of Eq. (1) combines ρ_∞ and V_∞, hence velocity must be known independently for atmospheric reconstruction. In the case of MSL, V_∞ was provided by IMU as described in [4].

Given values for C_{pt2}, V_∞, and p_∞, density can be reconstructed with Eq. (1). Atmospheric pressure and temperature may be derived from this density using

$$p_\infty = p_{BC} - \int_{r_{BC}}^{r} g(r)\rho_\infty(r)\,dr \tag{2a}$$

$$T_\infty = \frac{p_\infty}{\rho_\infty}\frac{m}{R} \tag{2b}$$

which express hydrostatic equilibrium and the ideal gas law, respectively. Eq. (2a) numerically integrates density over radial distance r from the center of Mars, using a spherical gravity model defined as $g(r) = g_0(r_0/r)^2$. The ideal gas law in Eq. (2b) contains the universal gas constant R and mean molecular weight m of the atmosphere, here taken constant at 0.044 kg/mol. Note atmospheric density and pressure are both included in Eq. (1) used to reconstruct ρ_∞, while p_∞ is derived from ρ_∞ with Eq. (2a).This was resolved with an iterative method that converges on when relative changes in reconstructed density are negligible. Most importantly, an equilibrium flow model is used to compute C_{pt2} in Eq. (1) as a function of velocity, atmospheric pressure, and temperature. This computation is repeated during every execution of the iterative loop containing Eq. (1–2), illustrated in Fig. 2.

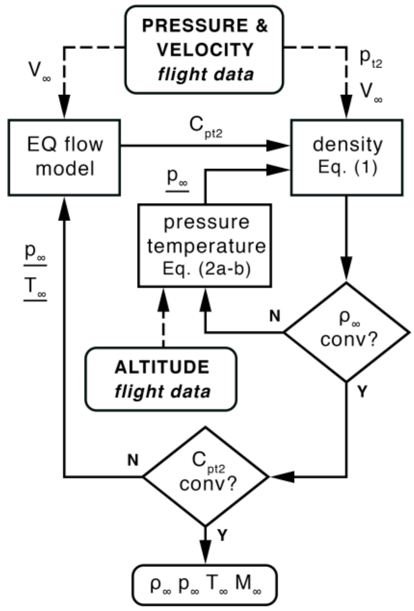

Fig. 2 Atmospheric reconstruction method with stagnation pressure, velocity, and altitude flight data (initial atmospheric values are underlined).

Conclusion:

This atmospheric reconstruction using stagnation pressure measurements of MSL, interpreted with a 1-D equilibrium flow model, closely agrees with results in literature that used pressure measurements from multiple heat shield pressure sensors, and using 3-D non-equilibrium Navier Stokes modeling. The present method is accurate to 1% in the hypersonic flight regime, and to at least 2% in the supersonic regime. The method can be applied to blunt vehicles of arbitrary geometry, and the pressure coefficients computed along the MSL trajectory are shown to be valid for a wide range of Mars entry missions. Application to ExoMars Schiaparelli data is in progress.

References:

[1] Blanchard, R. C., and Desai, P. N., "Mars Phoenix Entry, Descent, and Landing Trajectory and Atmosphere Reconstruction," Journal of Spacecraft and Rockets, Vol. 48, No. 5, 2011, pp. 809–821. doi:10.2514/1.46274

[2] Seiff, A., Reese, D. E., Jr., "Use of Entry Vehicle Responses to Define the Properties of the Mars Atmosphere," Advances in the Astronautical Sciences, Vol. 19, 1965, pp.419-447.

[3] Kutty, P., and Karlgaard, C., "Mars Science Laboratory Entry, Descent,and Landing Trajectory Reconstruction Uncertainty Assessment," 10th International Planetary Probe Workshop , San Jose, CA, June 2013.

[4] Karlgaard, C. D., Kutty, P., Schoenenberger, M., Shidner, J., and Munk, M., "Mars Entry Atmospheric Data System Trajectory Reconstruction Algorithms and Flight Results," AIAA 2013-0028, AIAA Aerospace Sciences Meeting, Grapevine, TX, 2013. doi: 10.2514/6.2013-28

[5] Karlgaard, C. D., Kutty, P., Schoenenberger, M., Munk, M., Little, A., Kuhl, and C. A., Shidner, J., "Mars Science Laboratory Entry Atmospheric Data System Trajectory and Atmosphere Reconstruction," Journal of Spacecraft and Rockets, Vol. 51, No. 4, 2014, pp. 1029–1047. doi: 10.2514/1.A32770

[6] Dutta, S., "Statistical methods for Reconstruction of Entry, Descent, and Landing Performance with Application to Vehicle Design," Ph.D. Dissertation, Daniel Guggenheim School of Aerospace Engineering, Georgia Institute of Technology, Atlanta, GA, 2013.

[7] Holmberg, N. A., Faust, R. P., and Holt, H. M., "Viking '75 Spacecraft Design and Test Summary, Volume 1 – Lander Design," NASA Reference Publication 1027, 1980.

[8] Euler, E. A., Adams, G. L., and Hopper, F. W., "Design and Reconstruction of the Viking Lander Descent Trajectories," Journal of Guidance and Control, Vol. 1, No. 5, 1978, pp. 372–378. doi:10.2514/3.55795

[9] Ingoldby, R. N., Michel, F. C., Flaherty, T. M., Doty, M. G., Preston, B., Villyard, K. W., and Steele, R. D., "Entry Data Analysis for Viking Landers," Contract report, NASA CR-159388, 1976.

[10] Blanchard, R. C., and Walberg, G. D., "Determination of the Hypersonic-Continuum/Rarefied-Flow Drag Coefficient of the Viking Lander Capsule 1 Aeroshell From Flight Data," Tech. report, NASA TM 1793, 1980.

[11] Dutta, S., "Statistical methods for Reconstruction of Entry, Descent, and Landing Performance with Application to Vehicle Design," Ph.D. Dissertation, Daniel Guggenheim School of Aerospace Engineering, Georgia Institute of Technology, Atlanta, GA, 2013.

[12] Edquist, K., "Computations of Viking Lander Capsule Hypersonic Aerodynamics with Comparisons to Ground and Flight data," AIAA-2006-6137, AIAA Atmospheric Flight Mechanics Conference and Exhibit, Keystone, CO, 2006.

[13] Karlgaard, C. D., Van Norman, J., and Siemers, P. M., "Mars Entry Atmospheric Data System Modeling, Calibration, and Error Analysis," Tech. Report, NASA TM-2014-218535.

[14] Cheatwood, F. M., Bose, D., Karlgaard, C. D., Kuhl, C. A., Santos, J. A., and Wright, M. J., "Mars Science Laboratory (MSL) Entry, Descent, and Landing Instrumentation (MEDLI): Complete Flight Data Set," Tech. Report, NASA TM-2014-218533.

[15] zur Nieden, P., and Olivier, H., "Determination of Atmospheric Densities from Reentry Flight Data," Journal of Spacecraft and Rockets, Vol. 44, No. 2, 2007, pp. 332–337.

doi: 10.2514/1.19338